Generalized Study of Dispersion-Induced Power Penalty Mitigation Techniques in Millimeter-Wave Fiber-Optic Links

J. M. Fuster, *Associate Member, IEEE*, J. Marti, *Member, IEEE*, J. L. Corral, *Associate Member, IEEE*, V. Polo, *Student Member, IEEE*, and F. Ramos, *Student Member, IEEE*

***Abstract*—The authors present a comprehensive analysis of the chromatic dispersion effects in harmonic upconverted millimeter-wave (mm-wave) fiber-optic links. The optical upconversion is performed through a photonic mixer based on a Mach–Zehnder electrooptical modulator. It is shown that by biasing the electrooptical modulator either at the maximum or at the minimum transmission bias points, the dispersion-induced power penalty effect on the upconverted signal may be sharply mitigated, which results in increasing the frequency-length product of the fiber-optic link. Experimental results are provided for the three different types of bias.**

***Index Terms*—Chromatic dispersion, electrooptical modulators, millimeter-wave fiber-optic links, photonic mixing.**

I. Introduction

THE GENERATION and transmission of microwave/millimeter-wave (mm-wave) signals using optics is highly desired in current applications involving hybrid photonic-microwave systems such as multipoint video distribution systems, remote antenna links and mobile communications microcellular systems [1], [2]. However, the performance of these systems is severely limited by the chromatic dispersion of standard single-mode fibers (SSMF) [3], which sharply limits the frequency-length product of fiber-optic links. To overcome this limitation several optical techniques such as chirped fiber gratings [4] and single sideband optical modulators [5] have been proposed. On the other hand, several harmonic upconverting fiber-optic link schemes based on Mach–Zehnder electrooptical modulators (MZ-EOM) have been proposed to alleviate the high-frequency/high-power requirements on the local oscillator (LO) source [6], [7]. The impact of biasing the MZ-EOM at the minimum transmission bias (MITB) point on the dispersion effects was theoretically outlined in [8], where it was shown that the dispersion-induced power penalty (DIPP) of the fiber-optic link may be sharply reduced when the second order harmonic of the LO source is considered to perform the harmonic upconversion. Recently, a 28-GHz LMDS fiber-optic link based on this technique, which transmits a 34-Mb/s signal through 73 km of SSMF with minor impact of fiber dispersion, has been demonstrated in [9].

Manuscript received March 24, 1999; revised January 7, 2000.

The authors are with ETSI Telecomunicacion, Universidad Politecnica de Valencia, Valencia 46071, Spain (e-mail: jfuster@dcom.upv.es; jmarti@dcom.upv.es).

Publisher Item Identifier S 0733-8724(00)03029-2.

In this paper, a generalized study on the effects of different MZ-EOM biasing types on the DIPP is presented. It is demonstrated that the DIPP in mm-wave optical links is alleviated when $2+4k$ LO harmonic orders, for $k=0,1,2,\ldots$, are used when MZ-EOM's are biased at the MITB point. Moreover, it is also reported on the DIPP mitigation feature for the $4+4k$ LO harmonic orders when MZ-EOM's are biased at the maximum transmission bias (MATB) point. Furthermore, we analyze the impact of the LO signal modulation index on the mitigation of the DIPP, which is shown that is a significant parameter when employing LO harmonics of order $\geq$4. We have recently reported the DIPP expressions for both the MITB and the MATB cases, assuming an optimum LO modulation index, which results in simpler expressions [10]. In this paper, we report the more complex and general expressions for both the MITB and the MATB cases.

The paper is organized as follows. In Section II, we present the general DIPP expressions for both the conventional and the upconverting schemes. In the upconverting case, all three modulation bias points: QB, MITB and MATB cases are considered. Section III is dedicated to understand the DIPP expressions derived in Section II from the interpretation of the MZ-EOM output field spectra. In Section IV, we analyze the influence of the LO modulation index on the DIPP. This section is repeatedly referred in Section II when reporting the simplifier DIPP expressions for the optimum values of the LO modulation index parameter. In Section V, an expression of the fiber-optic link bandwidth for the upconverting scheme is derived. Section VI presents experimental results which corroborates the theoretical analysis performed in the previous sections. Finally, conclusions are presented in Section VII.

II. Theoretical Analysis

Fig. 1 shows the setup of two different schemes of a mm-wave fiber-optic link: one based on a conventional RF-modulation scheme and the other based on an upconverting scheme. In the conventional system, the RF signal to be radiated by the antenna is externally modulated onto the optical carrier, as depicted in Fig. 1(a). Alternatively, an IF signal directly modulates the optical source in the upconverting system, and photonic upconversion is achieved through the LO signal driving the external modulator, as shown in Fig. 1(b). In both cases, the MZ-EOM output is launched into the optical fiber and may be optically amplified if necessary.

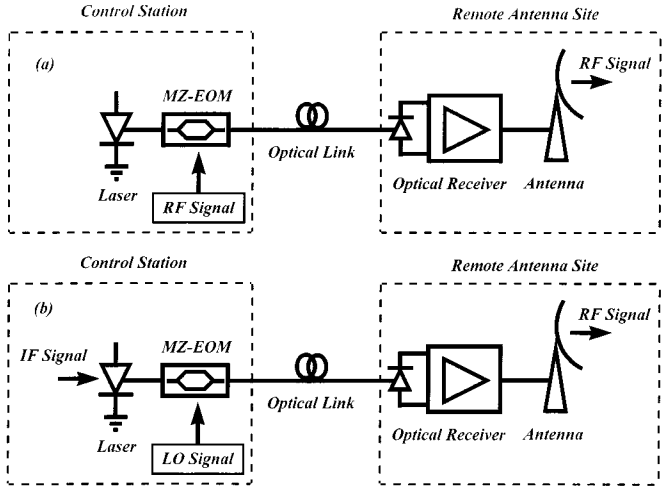

Fig. 1. Schematic of a mm-wave fiber-optic link. (a) Conventional modulating scheme (b) Upconverting scheme.

In the conventional link, fiber-optic chromatic dispersion affects the transmission of mm-wave signals [3]. The dispersion-induced power penalty (DIPP) of the fiber-optic link is defined as the power loss suffered by the photodetected signal due to the fiber chromatic dispersion effects. For a modulating signal at $f_{\rm RF}$ frequency, the DIPP of the fiber-optic link is given by

$$\begin{aligned}\mathrm{DIPP}^{\rm CONV} &= \frac{J_0\left(\frac{\alpha_{\rm RF}}{2}\right) J_1\left(\frac{\alpha_{\rm RF}}{2}\right)\cos\left(\beta f_{\rm RF}^2\right)}{J_0\left(\frac{\alpha_{\rm RF}}{2}\right) J_1\left(\frac{\alpha_{\rm RF}}{2}\right)} \\ &= \cos\left(\beta f_{\rm RF}^2\right) \end{aligned} \tag{1}$$

where $\beta = \pi D\lambda^2 L/c$ and $\alpha_{\rm RF} = \pi V_{\rm RF}/V_\pi(f_{\rm RF})$. $J_k(\cdot)$ stands for the kth-order Bessel function of the first kind. L and D are the length and the dispersion parameter of the optical fiber, respectively, λ is the optical wavelength and c is the speed of light in vacuum. $V_{\rm RF}$ and $V_\pi(f_{\rm RF})$ stand for the signal voltage and the half-wave voltage of the RF signal, respectively.

In the optically upconverted link, the RF signal frequency is given by $f_{\rm RF} = Nf_{\rm LO} + f_{\rm IF}$, where N is the LO harmonic order employed to perform the upconversion. In the next three subsections, we analyze the performance of the upconverting link for three different types of MZ-EOM bias: the quadrature bias (QB) point, the MITB point, and the MATB point. If the QB point is selected, the upconversion at the MZ-EOM device is performed through the odd harmonics of the LO driving signal ($N = 2k+1, k = 0, 1, 2, \ldots$). On the other hand, when biasing the MZ-EOM at either the MITB or the MATB points, the photonic mixing is carried out through the even harmonics of the LO signal ($N = 2k, k = 0, 1, 2, \ldots$).

A. MZ-EOM Biased at QB Point

When the MZ-EOM is biased at the QB point, the electrical field at the output of the MZ-EOM device ($E_{\rm EOM}^{\rm QB}$) is proportional to

$$\begin{aligned} E_{\rm EOM}^{\rm QB} &\propto E_{\rm laser}[1 + m_i\cos(\omega_{\rm IF}t)] \\ &\quad \times \cos\left[\frac{\pi}{4} + \frac{\alpha_{\rm LO}}{2}\cos(\omega_{\rm LO}t)\right] e^{j\omega_0 t} \\ &= \frac{E_{\rm laser}}{\sqrt{2}}[1 + m_i\cos(\omega_{\rm IF}t)] \\ &\quad \cdot \left[\sum_{k=-\infty}^{\infty}(-1)^k J_{2k}\left(\frac{\alpha_{\rm LO}}{2}\right)\cos(2k\omega_{\rm LO}t)\right. \\ &\quad \left. - \sum_{k=-\infty}^{\infty}(-1)^k J_{2k+1}\left(\frac{\alpha_{\rm LO}}{2}\right)\cos([2k+1]\omega_{\rm LO}t)\right] e^{j\omega_0 t} \\ &= \frac{E_{\rm laser}}{\sqrt{2}}\left[\sum_{k=-\infty}^{\infty}(-1)^k J_{2k}\left(\frac{\alpha_{\rm LO}}{2}\right)\cos(2k\omega_{\rm LO}t)\right. \\ &\quad - \sum_{k=-\infty}^{\infty}(-1)^k J_{2k+1}\left(\frac{\alpha_{\rm LO}}{2}\right)\cos([2k+1]\omega_{\rm LO}t) \\ &\quad + \frac{m_i}{2}\sum_{k=-\infty}^{\infty}(-1)^k J_{2k}\left(\frac{\alpha_{\rm LO}}{2}\right)\cos([2k\omega_{\rm LO} + \omega_{\rm IF}]t) \\ &\quad + \frac{m_i}{2}\sum_{k=-\infty}^{\infty}(-1)^k J_{2k}\left(\frac{\alpha_{\rm LO}}{2}\right)\cos([2k\omega_{\rm LO} - \omega_{\rm IF}]t) \\ &\quad - \frac{m_i}{2}\sum_{k=-\infty}^{\infty}(-1)^k J_{2k+1}\left(\frac{\alpha_{\rm LO}}{2}\right) \\ &\quad \times \cos([(2k+1)\omega_{\rm LO} + \omega_{\rm IF}]t) \\ &\quad - \frac{m_i}{2}\sum_{k=-\infty}^{\infty}(-1)^k J_{2k+1}\left(\frac{\alpha_{\rm LO}}{2}\right) \\ &\quad \left. \times \cos([(2k+1)\omega_{\rm LO} - \omega_{\rm IF}]t)\right] e^{j\omega_0 t} \end{aligned} \tag{2}$$

where $E_{\rm laser}$ is the laser electrical field, m_i is the laser modulation index, $\omega_{\rm IF} = 2\pi f_{\rm IF}, \omega_{\rm LO} = 2\pi f_{\rm LO}$, and $\alpha_{\rm LO} = \pi V_{\rm LO}/V_\pi(f_{\rm LO})$. $V_{\rm LO}$ and $V_\pi(f_{\rm LO})$ stand for the LO signal voltage and the half-wave voltage at the LO frequency, respectively.

After propagation through the optical fiber, the electrical field ($E_{\rm fiber}^{\rm QB}$) may be expressed as

$$\begin{aligned} E_{\rm fiber}^{\rm QB} &\propto \frac{E_{\rm laser}}{\sqrt{2}}\left[\sum_{k=-\infty}^{\infty}(-1)^k J_{2k}\left(\frac{\alpha_{\rm LO}}{2}\right)\right. \\ &\quad \times \cos(2k\omega_{\rm LO}t)e^{j\beta(2kf_{\rm LO})^2} \\ &\quad - \sum_{k=-\infty}^{\infty}(-1)^k J_{2k+1}\left(\frac{\alpha_{\rm LO}}{2}\right) \\ &\quad \times \cos([2k+1]\omega_{\rm LO}t)e^{j\beta([2k+1]f_{\rm LO})^2} \\ &\quad + \frac{m_i}{2}\sum_{k=-\infty}^{\infty}(-1)^k J_{2k}\left(\frac{\alpha_{\rm LO}}{2}\right) \\ &\quad \times \cos([2k\omega_{\rm LO} + \omega_{\rm IF}]t)e^{j\beta(2kf_{\rm LO}+f_{\rm IF})^2} \\ &\quad + \frac{m_i}{2}\sum_{k=-\infty}^{\infty}(-1)^k J_{2k}\left(\frac{\alpha_{\rm LO}}{2}\right) \\ &\quad \times \cos([2k\omega_{\rm LO} - \omega_{\rm IF}]t)e^{j\beta(2kf_{\rm LO}-f_{\rm IF})^2} \\ &\quad - \frac{m_i}{2}\sum_{k=-\infty}^{\infty}(-1)^k J_{2k+1}\left(\frac{\alpha_{\rm LO}}{2}\right) \\ &\quad \times \cos([(2k+1)\omega_{\rm LO} + \omega_{\rm IF}]t)e^{j\beta([2k+1]f_{\rm LO}+f_{\rm IF})^2} \\ &\quad - \frac{m_i}{2}\sum_{k=-\infty}^{\infty}(-1)^k J_{2k+1}\left(\frac{\alpha_{\rm LO}}{2}\right) \end{aligned}$$

$$\times \cos([(2k+1)\omega_{\rm LO} - \omega_{\rm IF}]t) \times e^{j\beta([2k+1]f_{\rm LO} - f_{\rm IF})^2} \Big] e^{j\omega_0 t} \quad (3)$$

The optical signal is then photodetected at the receiving end. From (3), it may be deduced that the RF component ($\omega_{\rm RF} = N\omega_{\rm LO} + \omega_{\rm IF}$) of the detected photocurrent is proportional to

$$i_{\rm phot}^{\rm QB} \propto RE_{\rm laser}^2 m_i \cos([N\omega_{\rm LO} + \omega_{\rm IF}]t) \cdot \sum_{k=0}^{N} J_k\left(\frac{\alpha_{\rm LO}}{2}\right) J_{N-k}\left(\frac{\alpha_{\rm LO}}{2}\right) \times \cos[\beta([N-k]f_{\rm LO} + f_{\rm IF})^2 - \beta(kf_{\rm LO})^2] \quad (4)$$

resulting in a DIPP factor given by (5) shown at the bottom of the page.

Equation (5) is a general expression that may be particularized for a certain LO odd harmonic. Thus, when fundamental photonic mixing is performed ($N = 1$) the DIPP factor may be expressed as,

$$\text{DIPP}_1^{\rm QB} = \cos(\beta f_{\rm IF} f_{\rm RF}) \cos(\beta f_{\rm LO} f_{\rm RF}) \quad (6)$$

Fig. 2 shows the $\text{DIPP}_1^{\rm QB}$ factor as a function of the RF signal frequency for three different values of the IF signal frequency (100 MHz, 1 GHz, and 2 GHz) and for 50 km of SSMF. As it may be observed from Fig. 2, the IF signal frequency governs the $\text{DIPP}_1^{\rm QB}$ envelope, as described by the factor $\cos(\beta f_{\rm IF} f_{\rm RF})$, while the term $\cos(\beta f_{\rm LO} f_{\rm RF})$, produces the "fast" fading behavior[1] of the $\text{DIPP}_1^{\rm QB}$. When a low IF signal frequency is considered ($f_{\rm IF} = 100$ MHz), $f_{\rm LO}$ tends to $f_{\rm RF}$, and the DIPP of the QB upconverting fiber-optic link approximates to that of the conventional case [see Fig. 2(a)].

Likewise, any particular expression of the DIPP for higher LO odd harmonics may be obtained from (5). Fig. 3 show the DIPP of the QB upconverting link as a function of the optical span for four different cases, in which the first, third, fifth and seventh LO odd harmonic are employed to perform the upconversion, respectively. The frequencies considered in the simulation have been 28 GHz and 1 GHz for the RF and the IF signals, respectively. It is worth to notice that although (5) becomes more complex as N increases, it will be shown in Section IV that the DIPP expressions may be simplify for certain values of the LO modulation index. In the QB case, this simplification results in a dominant term as

$$\text{DIPP}_N^{\rm QB} = \cos(\beta f_{\rm IF} f_{\rm RF}) \cos(\beta f_{\rm LO} f_{\rm RF}). \quad (7)$$

The different curves shown in Fig. 3 have been computed for the values of the LO modulation index that simplify the DIPP expression, as described in Section IV. These values are different for each case, because they depend on the order of the LO harmonic employed in the upconversion process.

As it may be observed from Fig. 3, the DIPP results for all four cases present the same envelope defined by the first cosine term in (7), i.e., $\cos(\beta f_{\rm IF} f_{\rm RF})$. The second cosine function, $\cos(\beta f_{\rm LO} f_{\rm RF})$, governs the "fast" fading behavior of the DIPP results, and it is different in each case as the LO signal frequency is given by $f_{\rm LO} = (f_{\rm RF} - f_{\rm IF})/N$, as it is shown in Fig. 3.

[1]Fast fading in terms of the frequency-length product.

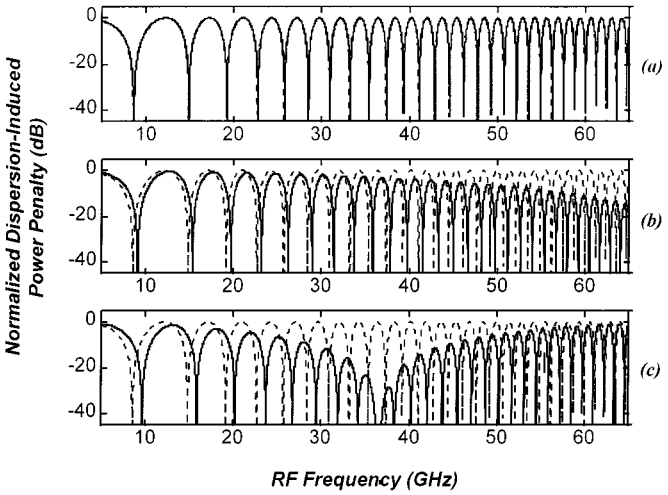

Fig. 2. DIPP against the RF signal frequency for the conventional modulating case (dashed line) and the upconverting ($N = 1$) QB case (solid line). (a) $f_{\rm IF} = 100$ MHz (b) $f_{\rm IF} = 1$ GHz (c) $f_{\rm IF} = 2$ GHz.

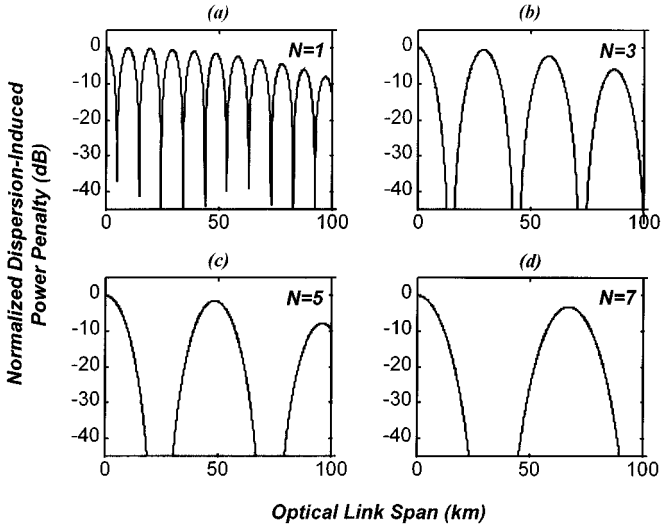

Fig. 3. DIPP against the optical span for the upconverting QB case. $f_{\rm IF} = 1$ GHz, $f_{\rm RF} = 28$ GHz. (a) $N = 1$ (b) $N = 3$ (c) $N = 5$ (d) $N = 7$.

$$\text{DIPP}_N^{\rm QB} = \frac{\sum_{k=0}^{N} J_k\left(\frac{\alpha_{\rm LO}}{2}\right) J_{N-k}\left(\frac{\alpha_{\rm LO}}{2}\right) \cos[\beta([N-k]f_{\rm LO} + f_{\rm IF})^2 - \beta(kf_{\rm LO})^2]}{\sum_{k=0}^{N} J_k\left(\frac{\alpha_{\rm LO}}{2}\right) J_{N-k}\left(\frac{\alpha_{\rm LO}}{2}\right)}. \quad (5)$$

B. MZ-EOM Biased at MITB Point

If the MZ-EOM is biased at the MITB point, the electrical field at the output of the MZ-EOM device ($E_{\rm EOM}^{\rm MITB}$) is proportional to

$$\begin{aligned}E_{\rm EOM}^{\rm MITB} &\propto E_{\rm laser}[1+m_i\cos(\omega_{\rm IF}t)]\\ &\quad\times\cos\left[\frac{\pi}{2}+\frac{\alpha_{\rm LO}}{2}\cos(\omega_{\rm LO}t)\right]e^{j\omega_0 t}\\ &= E_{\rm laser}[1+m_i\cos(\omega_{\rm IF}t)]\\ &\quad\times\left[\sum_{k=-\infty}^{\infty}(-1)^k J_{2k+1}\left(\frac{\alpha_{\rm LO}}{2}\right)\right.\\ &\quad\left.\times\ \cos([2k+1]\omega_{\rm LO}t)\right]e^{j\omega_0 t}\\ &= E_{\rm laser}\left[\sum_{k=-\infty}^{\infty}(-1)^k J_{2k+1}\left(\frac{\alpha_{\rm LO}}{2}\right)\right.\\ &\quad\times\cos([2k+1]\omega_{\rm LO}t)\\ &\quad+\frac{m_i}{2}\sum_{k=-\infty}^{\infty}(-1)^k J_{2k+1}\left(\frac{\alpha_{\rm LO}}{2}\right)\\ &\quad\times\cos([(2k+1)\omega_{\rm LO}+\omega_{\rm IF}]t)\\ &\quad+\frac{m_i}{2}\sum_{k=-\infty}^{\infty}(-1)^k J_{2k+1}\left(\frac{\alpha_{\rm LO}}{2}\right)\\ &\quad\left.\times\cos([(2k+1)\omega_{\rm LO}-\omega_{\rm IF}]t)\right]e^{j\omega_0 t}. \qquad (8)\end{aligned}$$

After propagation through the optical fiber, the electrical field ($E_{\rm fiber}^{\rm MITB}$) may be expressed as

$$\begin{aligned}E_{\rm fiber}^{\rm MITB} &\propto E_{\rm laser}\left[\sum_{k=-\infty}^{\infty}(-1)^k J_{2k+1}\left(\frac{\alpha_{\rm LO}}{2}\right)\right.\\ &\quad\times\cos([2k+1]\omega_{\rm LO}t)e^{j\beta([2k+1]f_{\rm LO})^2}\\ &\quad+\frac{m_i}{2}\sum_{k=-\infty}^{\infty}(-1)^k J_{2k+1}\left(\frac{\alpha_{\rm LO}}{2}\right)\\ &\quad\times\cos([(2k+1)\omega_{\rm LO}+\omega_{\rm IF}]t)e^{j\beta([2k+1]f_{\rm LO}+f_{\rm IF})^2}\\ &\quad+\frac{m_i}{2}\sum_{k=-\infty}^{\infty}(-1)^k J_{2k+1}\left(\frac{\alpha_{\rm LO}}{2}\right)\\ &\quad\times\cos([(2k+1)\omega_{\rm LO}-\omega_{\rm IF}]t)\\ &\quad\left.e^{j\beta([2k+1]f_{\rm LO}-f_{\rm IF})^2}\right]e^{j\omega_0 t}. \qquad (9)\end{aligned}$$

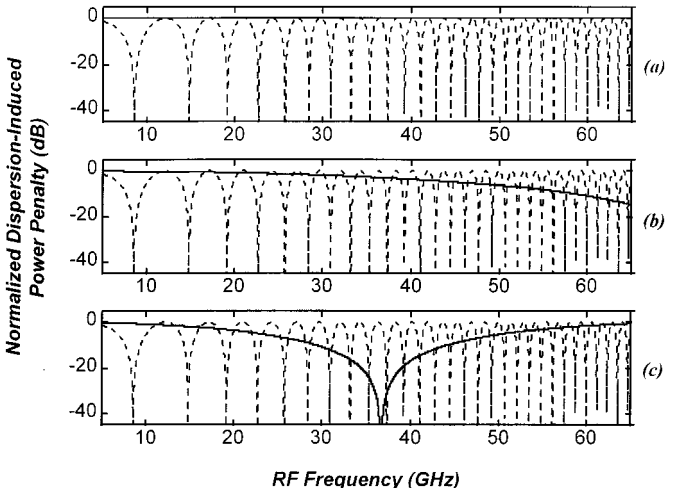

Fig. 4. DIPP against the RF signal frequency for the conventional modulating case (dashed line) and the upconverting ($N=2$) MITB case (solid line). (a) $f_{\rm IF}=100$ MHz. (b) $f_{\rm IF}=1$ GHz. (c) $f_{\rm IF}=2$ GHz.

The optical signal is then photodetected at the receiving end. From (9), it may be deduced that the RF component of the detected photocurrent is proportional to

$$\begin{aligned}i_{\rm phot}^{\rm MITB} &\propto RE_{\rm laser}^2 m_i\cos([N\omega_{\rm LO}+\omega_{\rm IF}]t)\\ &\quad\cdot\sum_{k=0}^{N/2-1}J_{2k+1}\left(\frac{\alpha_{\rm LO}}{2}\right)J_{N-2k-1}\left(\frac{\alpha_{\rm LO}}{2}\right)\\ &\quad\times\cos[\beta([N-2k-1]f_{\rm LO}+f_{\rm IF})^2\\ &\quad-\beta([2k+1]f_{\rm LO})^2] \qquad (10)\end{aligned}$$

resulting in a DIPP factor given by (11) shown at the bottom of the page.

When the upconversion is performed through the second harmonic of the LO driving signal, (11) may be expressed as

$$\text{DIPP}_2^{\rm MITB}=\cos[\beta f_{\rm IF}f_{\rm RF}]. \qquad (12)$$

Fig. 4 depicts the DIPP of a 50-km fiber-optic link as a function of the RF signal frequency for the same cases ($f_{\rm IF}=100$ MHz, $f_{\rm IF}=1$ GHz, $f_{\rm IF}=2$ GHz) considered in Fig. 2, but employing the LO second harmonic and MITB at the MZ-EOM. As may be observed from Fig. 4, the DIPP results for MITB fit the envelopes of the results obtained for QB (depicted in Fig. 2), as predicted by (12). MITB results depicted in Fig. 4 show significant improvement of the fiber-optic link bandwidth. Moreover, it may be observed from Fig. 4 that the magnitude of the improvement inversely depends on the IF signal frequency.

In Fig. 5, it is shown the DIPP for the MITB case as a function of the optical span, when the upconversion is performed through the second, fourth, sixth or eighth harmonic of the LO driving signal. The IF and RF frequencies are 1 GHz and 28 GHz, respectively. As for the QB case, (11) may be simplified

$$\text{DIPP}_N^{\rm MITB}=\frac{\sum_{k=0}^{N/2-1}J_{2k+1}\left(\frac{\alpha_{\rm LO}}{2}\right)J_{N-2k-1}\left(\frac{\alpha_{\rm LO}}{2}\right)\cos[\beta([N-2k-1]f_{\rm LO}+f_{\rm IF})^2-\beta([2k+1]f_{\rm LO})^2]}{\sum_{k=0}^{N/2-1}J_{2k+1}\left(\frac{\alpha_{\rm LO}}{2}\right)J_{N-2k-1}\left(\frac{\alpha_{\rm LO}}{2}\right)}. \qquad (11)$$

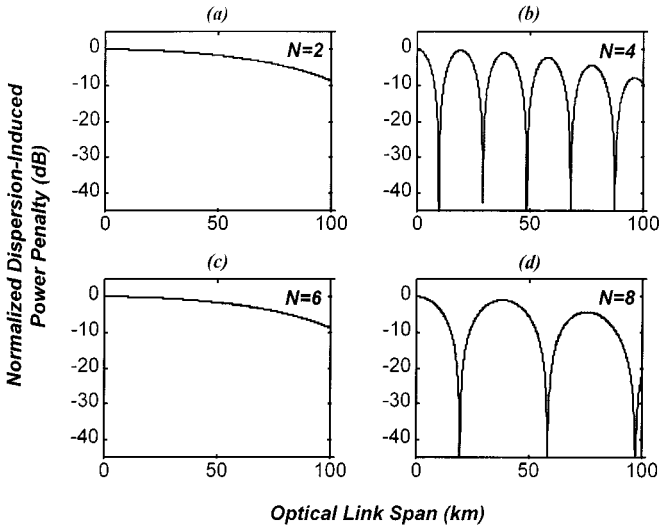

Fig. 5. DIPP against the optical span for the upconverting MITB case. $f_{\rm IF} = 1$ GHz, $f_{\rm RF} = 28$ GHz. (a) $N = 2$. (b) $N = 4$. (c) $N = 6$. (d) $N = 8$.

for certain LO modulation indexes (Section IV). Thus, when photonic mixing is carried out with a LO harmonic of order $2 + 4k, k = 0, 1, 2, \ldots$, the DIPP may be expressed as

$$\mathrm{DIPP}^{\rm MITB}_{N=2+4k} \approx \cos[\beta f_{\rm IF} f_{\rm RF}]. \tag{13}$$

On the other hand, when employing LO harmonics of order $4 + 4k, k = 0, 1, 2, \ldots$, the DIPP is given by,

$$\mathrm{DIPP}^{\rm MITB}_{N=4+4k} \approx \cos[\beta f_{\rm IF} f_{\rm RF}] \cos[2\beta f_{\rm LO} f_{\rm RF}]. \tag{14}$$

As may be observed from Fig. 5, the DIPP results for the cases $N = 2$ and $N = 6$, i.e., LO harmonics of orders $2 + 4k$, correspond to the envelope defined by $\cos(\beta f_{\rm IF} f_{\rm RF})$, as predicted by (13). Likewise, the DIPP curves of the cases $N = 4$ and $N = 8$, LO harmonics of order $4+4k$, are governed by (14). The differences between the results shown for the $N = 4$ and $N = 8$ cases are only due to the different LO signal frequency employed in each case.

C. MZ-EOM Biased at MATB Point

When the MZ-EOM is biased at the MATB point, the electrical field at the output of the MZ-EOM device ($E^{\rm MATB}_{\rm EOM}$) is proportional to

$$\begin{aligned} E^{\rm MATB}_{\rm EOM} &\propto E_{\rm laser}[1 + m_i \cos(\omega_{\rm IF} t)] \\ &\quad \times \cos\left[\frac{\alpha_{\rm LO}}{2}\cos(\omega_{\rm LO} t)\right] e^{j\omega_0 t} \\ &= E_{\rm laser}[1 + m_i \cos(\omega_{\rm IF} t)] \\ &\quad \times \left[\sum_{k=-\infty}^{\infty} (-1)^k J_{2k}\left(\frac{\alpha_{\rm LO}}{2}\right)\cos(2k\omega_{\rm LO} t)\right] e^{j\omega_0 t} \\ &= E_{\rm laser}\left[\sum_{k=-\infty}^{\infty} (-1)^k J_{2k}\left(\frac{\alpha_{\rm LO}}{2}\right)\cos(2k\omega_{\rm LO} t)\right. \\ &\quad + \frac{m_i}{2}\sum_{k=-\infty}^{\infty} (-1)^k J_{2k}\left(\frac{\alpha_{\rm LO}}{2}\right) \\ &\quad \times \cos([2k\omega_{\rm LO} + \omega_{\rm IF}]t) \\ &\quad + \frac{m_i}{2}\sum_{k=-\infty}^{\infty} (-1)^k J_{2k}\left(\frac{\alpha_{\rm LO}}{2}\right) \\ &\quad \left.\times \cos([2k\omega_{\rm LO} - \omega_{\rm IF}]t)\right] e^{j\omega_0 t}. \end{aligned} \tag{15}$$

After propagation through the optical fiber, the electrical field ($E^{\rm MATB}_{\rm fiber}$) may be expressed as

$$\begin{aligned} E^{\rm MATB}_{\rm fiber} &\propto E_{\rm laser}\left[\sum_{k=-\infty}^{\infty} (-1)^k J_{2k}\left(\frac{\alpha_{\rm LO}}{2}\right)\right. \\ &\quad \times \cos(2k\omega_{\rm LO} t) e^{j\beta(2kf_{\rm LO})^2} \\ &\quad + \frac{m_i}{2}\sum_{k=-\infty}^{\infty} (-1)^k J_{2k}\left(\frac{\alpha_{\rm LO}}{2}\right) \\ &\quad \times \cos([2k\omega_{\rm LO} + \omega_{\rm IF}]t) e^{j\beta(2kf_{\rm LO}+f_{\rm IF})^2} \\ &\quad + \frac{m_i}{2}\sum_{k=-\infty}^{\infty} (-1)^k J_{2k}\left(\frac{\alpha_{\rm LO}}{2}\right) \\ &\quad \left.\times \cos([2k\omega_{\rm LO} - \omega_{\rm IF}]t) e^{j\beta(2kf_{\rm LO}-f_{\rm IF})^2}\right] e^{j\omega_0 t}. \end{aligned} \tag{16}$$

The optical signal is then photodetected at the receiving end. From (16), it may be deduced that the RF component of the detected photocurrent is proportional to

$$\begin{aligned} i^{\rm MATB}_{\rm phot} &= RE^2_{\rm laser} m_i \cos([N\omega_{\rm LO} + \omega_{\rm IF}]t) \\ &\quad \cdot \sum_{k=0}^{N/2} J_{2k}\left(\frac{\alpha_{\rm LO}}{2}\right) J_{N-2k}\left(\frac{\alpha_{\rm LO}}{2}\right) \\ &\quad \times \cos[\beta([N-2k]f_{\rm LO} + f_{\rm IF})^2 - \beta(2kf_{\rm LO})^2] \end{aligned} \tag{17}$$

resulting in a DIPP factor given by (18) shown at the bottom of the next page.

Fig. 6 depicts the DIPP for the MATB case as a function of the optical span, when photonic mixing is performed through the second, fourth, sixth or eighth harmonic of the LO driving signal. As for the QB and MITB cases, the IF and RF signal frequencies are 1 GHz and 28 GHz, respectively, and (18) may be simplified for certain LO modulation indexes (Section IV). When upconversion is performed through LO harmonics of order $4 + 4k$, the DIPP may be expressed as

$$\mathrm{DIPP}^{\rm MITB}_{N=4+4k} \approx \cos[\beta f_{\rm IF} f_{\rm RF}] \tag{19}$$

while when employing LO harmonics of $2 + 4k$, the DIPP is simplify to

$$\mathrm{DIPP}^{\rm MATB}_{N=2+4k} \approx \cos[\beta f_{\rm IF} f_{\rm RF}] \cos[2\beta f_{\rm LO} f_{\rm RF}]. \tag{20}$$

As it may be observed from Fig. 6, the DIPP results for the $N = 4$ and $N = 8$ cases, i.e., LO harmonics of order $4 + 4k$, correspond to the envelope defined by $\cos(\beta f_{\rm IF} f_{\rm RF})$, as predicted by (19). The DIPP results for the $N = 2$ and $N = 6$ cases, i.e., LO harmonics of order $2+4k$, are governed by (20). The differences between the results shown for the $N = 2$ and

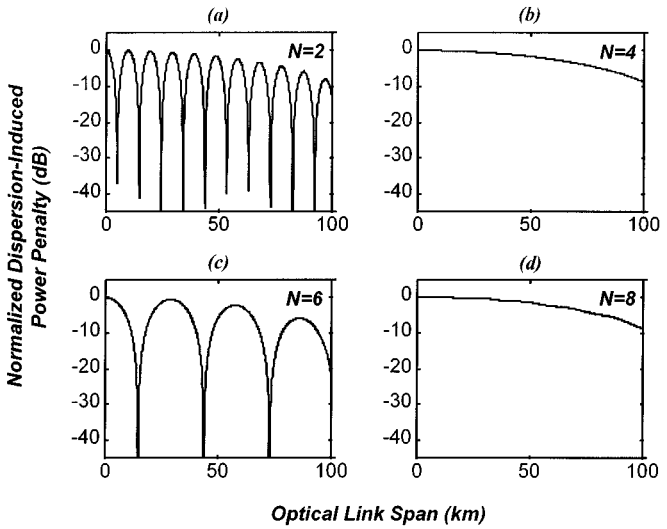

Fig. 6. DIPP against the optical span for the upconverting MATB case. $f_{\mathrm{IF}} = 1$ GHz, $f_{\mathrm{RF}} = 28$ GHz. (a) $N = 2$ (b) $N = 4$ (c) $N = 6$ (d) $N = 8$.

$N = 6$ cases are only due to the different LO signal frequency employed in each case.

III. Discussion on the MZ-EOM Output Optical Field Spectra

To explain the dispersion tolerant transmission achieved when biasing the MZ-EOM at MATB, the optical field spectra at the output of the MZ-EOM is considered. A similar explanation may be provided when the MZ-EOM is biased at the MITB point [10], which corresponds to DIPP expressions given by (13) and (14). Fig. 7 depicts the optical field spectra when the MZ-EOM is biased at the MATB point. In Fig. 7(a), the RF signal is generated as optical harmonic mixing the IF signal with the fourth harmonic of the LO driving signal (fourth-harmonic case), while spectra shown in Fig. 7(b) are for the case in which upconversion is carried out through the LO second harmonic (second-harmonic case). In both cases, the pairs of frequency components that primarily contribute when heterodyning to the RF signal are remarked using arrows. For the fourth-harmonic case, it should be pointed out that the relative frequency between the two beating terms which generate the $4f_{\mathrm{LO}} + f_{\mathrm{IF}}$ frequency is f_{IF}, which governs the DIPP in this case, as derived in (19) for $k = 0$. For the second-harmonic case, the relative frequencies among the spectral components that generate the $2f_{\mathrm{LO}} + f_{\mathrm{IF}}$ term are $2f_{\mathrm{LO}}$ and f_{IF}, which govern the two cosine functions of the corresponding DIPP, as stated in (20) for $k = 0$. When higher order harmonics of the LO driving signal are considered, the principal frequency components are distributed either as in Fig. 7(a) (order $4 + 4k, k = 0, 1, 2, \ldots$) or as in Fig. 7(b) (order $2 + 4k, k = 0, 1, 2, \ldots$), and the corresponding DIPP are the same as those obtained for the fourth-harmonic case and the second-harmonic case, respectively.

IV. Influence of the LO Modulation Index on the Dispersion-Induced Power Penalty

As stated in Section II, the expression of the DIPP strongly depends on the LO modulation index. This dependence is due to the DIPP being the sum of several terms for even harmonics of orders $N \geq 6$ and orders $N \geq 4$ for the MITB and MATB cases, respectively. Provided that the appropriate bias to reduce the DIPP of the upconverting link is chosen, i.e., MITB for LO harmonics of order $2 + 4k$ and MATB for LO harmonics of order $4 + 4k$, the DIPP will be composed by the sum of the desired term, $\cos(\beta f_{\mathrm{IF}} f_{\mathrm{RF}})$, and other undesired terms. The aim of choosing properly the LO modulation index is to minimize the influence of the undesired terms. Thus, if upconversion through the sixth harmonic of the LO driving signal with MITB bias is considered, the DIPP expression may be calculated from (11), and is given by (21) shown at the bottom of the page.

In this case, the desired term is governed by two third-order bessel functions $(J_3 \cdot J_3)$, while the unique undesired term is governed by the product of a first and a fifth-order bessel functions $(J_1 \cdot J_5)$. Fig. 8 depicts the amplitudes of the two DIPP terms stated in (21). In Fig. 8(a), a low LO modulation index is chosen, and the amplitude of both terms is very similar. As shown in Fig. 8(b), with the chosen value of the LO modulation index the undesired term affects the DIPP, producing an annoying ripple over the desired curve. This ripple may be eliminated by a properly choose of the LO modulation index. In Fig. 8(c), the LO modulation index is chosen to suppress the undesired term, which results in a DIPP free of any ripple [Fig. 8(d)]. As the LO harmonic order increases, the number of undesired terms of the DIPP factor becomes higher. In these cases is not possible to achieve a complete suppression of all the undesired terms. The choosing of the LO modulation index is based on achieving the maximum span between the amplitudes of the desire term and the sum of undesired terms, which coincides with the LO modulation index for which the main undesired term is suppressed. Although a minimum ripple

$$\mathrm{DIPP}_N^{\mathrm{MATB}} = \frac{\sum_{k=0}^{N/2} J_{2k}\left(\frac{\alpha_{\mathrm{LO}}}{2}\right) J_{N-2k}\left(\frac{\alpha_{\mathrm{LO}}}{2}\right) \cos[\beta([N-2k]f_{\mathrm{LO}} + f_{\mathrm{IF}})^2 - \beta(2kf_{\mathrm{LO}})^2]}{\sum_{k=0}^{N/2} J_{2k}\left(\frac{\alpha_{\mathrm{LO}}}{2}\right) J_{N-2k}\left(\frac{\alpha_{\mathrm{LO}}}{2}\right)}. \tag{18}$$

$$\mathrm{DIPP}_6^{\mathrm{MITB}} = \frac{J_1\left(\frac{\alpha_{\mathrm{LO}}}{2}\right) J_5\left(\frac{\alpha_{\mathrm{LO}}}{2}\right) \cos(\beta f_{\mathrm{IF}} f_{\mathrm{RF}}) \cos(4\beta f_{\mathrm{LO}} f_{\mathrm{RF}}) + J_3\left(\frac{\alpha_{\mathrm{LO}}}{2}\right) J_3\left(\frac{\alpha_{\mathrm{LO}}}{2}\right) \cos(\beta f_{\mathrm{IF}} f_{\mathrm{RF}})}{J_1\left(\frac{\alpha_{\mathrm{LO}}}{2}\right) J_5\left(\frac{\alpha_{\mathrm{LO}}}{2}\right) + J_3\left(\frac{\alpha_{\mathrm{LO}}}{2}\right) J_3\left(\frac{\alpha_{\mathrm{LO}}}{2}\right)}. \tag{21}$$

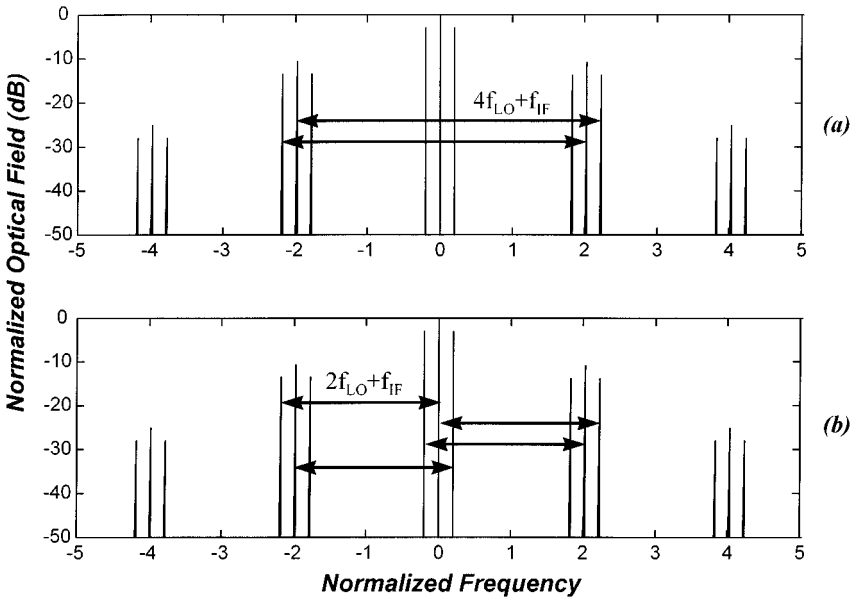

Fig. 7. Simulated optical field spectra at the output of the MZ-EOM device for the MATB case, as a function of the normalized frequency. (a) $f_{\mathrm{RF}} = 4f_{\mathrm{LO}} + f_{\mathrm{IF}}$ (b) $f_{\mathrm{RF}} = 2f_{\mathrm{LO}} + f_{\mathrm{IF}}$.

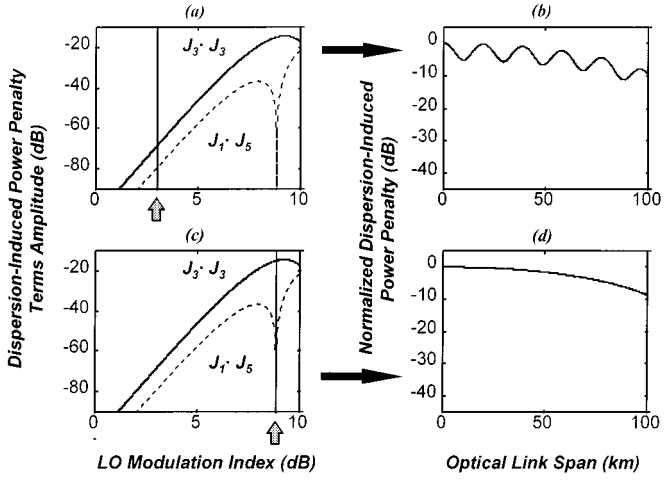

Fig. 8. Selection of the optimum LO modulation index for the MITB case with $N = 6$. $f_{\mathrm{IF}} = 1$ GHz, $f_{\mathrm{RF}} = 28$ GHz. (a) & (c) Amplitude of the DIPP terms against the LO modulation index. (a) Nonoptimum LO modulation index (c) Nonoptimum LO modulation index (b) and (d) DIPP against the optical link span. (b) Non-optimum LO modulation index. (d) Nonoptimum LO modulation index.

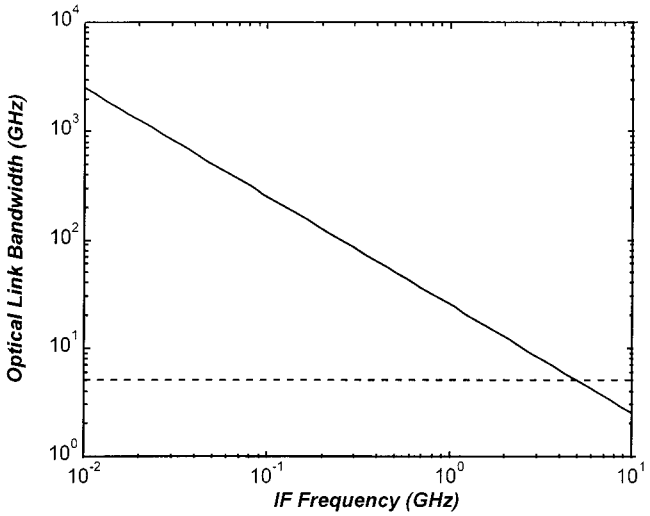

Fig. 9. Optical link bandwidth against the IF signal frequency for the conventional modulating case (dashed line) and the upconverting MITB/MATB cases (solid line). The optical span is 73 km.

remains in these situations, it is completely negligible as it may be observed in Fig. 6(d).

V. Fiber-Optic Link Bandwidth

The -3-dB bandwidth $(\Delta f_{-3\,\mathrm{dB}})$ of the optical link may be defined as the RF frequency at which the DIPP falls 3 dB due to the fiber chromatic dispersion. $\Delta f_{-3\,\mathrm{dB}}$ may be calculated for both the conventional and the upconverting cases. In the conventional modulating case, $\Delta f_{-3\,\mathrm{dB}}$ may be deduced from (1) and it is found to be $\Delta f_{-3\,\mathrm{dB}}^{\mathrm{CONV}} = \sqrt{\pi/4\beta}$. When the DIPP is reduced in the MITB/MATB upconverting cases ($\mathrm{DIPP}_{N=2+4k}^{\mathrm{MITB}}$ and $\mathrm{DIPP}_{N=4+4k}^{\mathrm{MATB}}$), $\Delta f_{-3\,\mathrm{dB}}$ may be calculated from either (11) or (16) and is given by $\Delta f_{-3\,\mathrm{dB}}^{\mathrm{UC}} = \pi/4\beta f_{\mathrm{IF}}$ for both cases. Fig. 9 shows the $\Delta f_{-3\,\mathrm{dB}}$ against the IF signal frequency for an optical span of 73 km. As it can be seen in Fig. 9, the optical link -3 dB bandwidth of the conventional modulating case does not depend on the IF signal frequency, while for the upconverting case it inversely depends on f_{IF}. Thus, for a f_{IF} of 1 GHz the link bandwidth for the modulating case is approximately 5 GHz, while it increases over 25 GHz for the upconverting case. If a lower f_{IF} of 100 MHz is used, the $\Delta f_{-3\,\mathrm{dB}}^{\mathrm{CONV}}$ remains at 5 GHz, while the $\Delta f_{-3\,\mathrm{dB}}^{\mathrm{UPCONV}}$ is extended further 250 GHz, which results in a mm-wave transmission free from the carrier suppression effect due to fiber chromatic dispersion.

VI. Experimental Results

Fig. 10 depicts the experimental measurement (circles) of the DIPP as a function of the RF signal frequency for four different cases. A 500-MHz IF signal frequency and a 73-km

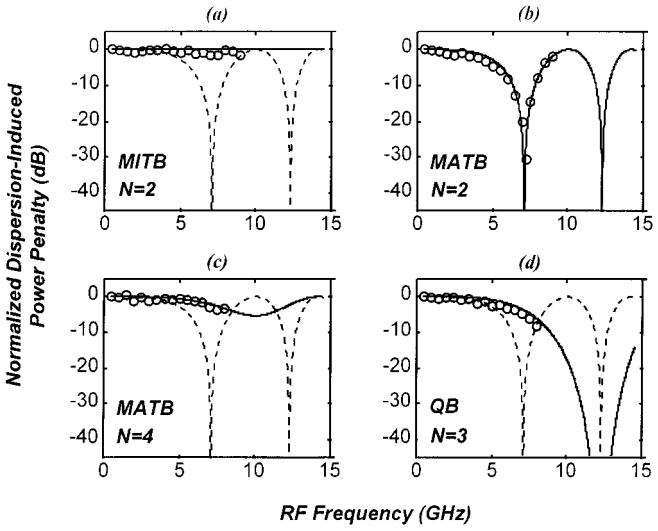

Fig. 10. DIPP against the RF signal frequency: conventional case simulation (dashed line), upconverting case simulation (solid line), upconverting case experiments (circles). The optical span is 73 km and $f_{\mathrm{IF}} = 500$ MHz. (a) MITB, $N = 2$. (b) MATB, $N = 2$. (c) MATB, $N = 4$. (d) QB, $N = 3$.

fiber-optic link span have been employed in all the measurements. In Fig. 10(a), it may be observed that the DIPP is effectively mitigated by employing the second LO harmonic order with the MZ-EOM biased at MITB. In contrast, the DIPP is not reduced when employing the same LO harmonic, but with the MZ-EOM biased at MATB [Fig. 10(b)]. Fig. 10(c) shows that a significant reduction of the DIPP is also achieved in the MATB case, by employing the fourth harmonic order of the LO driving signal. Moreover, the ripple predicted by theory is observed in Fig. 10(c), as the LO modulation index employed in the experiment was not the optimum value. Finally, Fig. 10(d) shows the DIPP measurements corresponding to the upconverting QB case, when employing the third harmonic of the LO signal. All four measurements are compared with their theoretic results (solid lines) and with the DIPP of the conventional modulator (dashed line). In the experiments we have also noticed that the biasing deviation around either the MITB or the MATB points seriously influences on the mitigation of the DIPP, and a bias control circuit is necessary to ensure biasing at the exact MITB or MATB points.

VII. Conclusion

In this paper we have presented a comprehensive analysis of the dispersion-induced power penalty mitigation techniques in mm-wave fiber-optic links, which are based on biasing the upconverting MZ-EOM at the nonlinear points: MITB and MATB. When these techniques are employed, the optical link bandwidth is significantly increased. For example, in a conventional modulating link of 73-km fiber span, the optical link bandwidth is 5 GHz. If either MITB or MATB upconversion is employed, the optical link bandwidth is extended further 50 GHz for an IF signal of 500 MHz, improving the $\Delta f_{-3\,\mathrm{dB}}$ in a factor of 10. The potential improvement of the proposed techniques depend on the value of the IF signal frequency. If a lower IF signal of 100 MHz is considered, the $\Delta f_{-3\,\mathrm{dB}}$ is theoretically spanned over 250 GHz. Additionally, the MITB and MATB upconverting techniques proposed in this paper require LO driving signals of lower frequencies, which result in simpler and more economical electronics. The LO signal frequency required in the upconverting case is that of the conventional case divided by the order of the LO harmonic employed in the upconversion. Therefore, both the MITB and MATB upconverting links are proposed as an alternative to the conventional modulating optical link for mm-wave transmission in antenna remoting systems.

Acknowledgment

The authors would like to thank the anonymous reviewers for their fruitful comments.

References

[1] S. Komaki, K. Tsukamoto, and M. Okada, "Requirements for radio-wave photonic devices from the viewpoint of future mobile radio system," *IEEE Trans. Microwave Theory Tech.*, vol. 43, pp. 2222–2228, 1995.

[2] J. Park, A. F. Elrefaie, and K. Y. Lau, "1550 nm transmission of digitally modulated 28 GHz subcarriers over 77 km of nondispersion shifted fiber," *IEEE Photon. Technol. Lett.*, vol. 9, pp. 256–258, 1998.

[3] H. Schmuck, "Comparison of optically millimeter-wave system concepts with regard to chromatic dispersion," *Electron. Lett.*, vol. 31, pp. 1848–1849, 1995.

[4] J. Marti, J. M. Fuster, and R. I. Laming, "Experimental reduction of chromatic dispersion effects in lightwave microwave/millimeter-vawe transmissions employing tapered linearly chirped fiber gratings," *Electron. Lett.*, vol. 33, pp. 1170–1171, 1997.

[5] G. H. Smith, D. Novak, and Z. Ahmed, "Technique for optical SSB generation to overcome fiber dispersion penalties in fiber-radio systems," *Electron. Lett.*, vol. 33, pp. 74–75, 1997.

[6] C. K. Sun, R. J. Orazi, S. A. Pappert, and W. K. Burns, "A photonic-link millimeter-wave mixer using cascaded optical modulators and harmonic carrier generation," *IEEE Photon. Technol. Lett.*, vol. 8, pp. 1166–1168, 1996.

[7] G. P. Gopalakrishnan, W. K. Burns, and C. H. Bulmer, "Microwave-optical mixing in $LiNbO_3$ modulators," *IEEE Trans. Microwave Theory Tech.*, vol. 41, pp. 2383–2391, 1993.

[8] J. M. Fuster, J. Marti, and J. L. Corral, "Chromatic dispersion effects in electro-optical up-converted millimeter-wave fiber-optic links," *Electron. Lett.*, vol. 33, pp. 1969–1970, 1997.

[9] V. Polo, F. Ramos, J. Marti, and J. M. Fuster, "Demonstration of dispersion-tolerant 34 Mbit/s data transmission in electro-optically upconverted 28 GHz LMDS fiber-optic link," presented at the IEEE MTT-S Int. Microwave Symp., Anaheim, CA, 1999.

[10] J. M. Fuster, J. Marti, V. Polo, F. Ramos, and J. L. Corral, "Mitigation of dispersion-induced power penalty in millimeter-wave fiber-optic links," *Electron. Lett.*, vol. 34, pp. 1869–1870, 1998.

J. M. Fuster (A'98), photograph and biography not available at the time of publication.

J. Marti (S'89–M'92), photograph and biography not available at the time of publication.

J. L. Corral (A'98), photograph and biography not available at the time of publication.

V. Polo (S'99), photograph and biography not available at the time of publication.

F. Ramos (S'99), photograph and biography not available at the time of publication.